ELSEVIER

Journal of Nuclear Materials 266–269 (1999) 593–597

journal of nuclear materials

Runaway-limiter interaction in the FTU tokamak during disruptions

G. Maddaluno *, B. Esposito

Associazione EURATOM ENEA sulla Fusione, CRE Frascati, C.P. 65, 00044 Frascati, Rome, Italy

Abstract

Photoneutron production during disruptions was monitored on the FTU machine by a set of calibrated BF_3 proportional counters. Both hydrogen and deuterium discharges covering a wide density range were examined. The functional dependence of the photoneutron production on n_e, Z_{eff} and I_p is in agreement with the Dreicer generation, being the main source of runaway electrons during disruptions in FTU. No detectable photoneutron production was observed at a plasma density higher than 1.4×10^{20} m^{-3}, corresponding to Z_{eff} values close to 1. The typical runaway energy was evaluated from the curve of the photoneutron yield per electron vs. energy for disruptions characterized by a hesitation in the plasma current decay. Damage by disruption generated runaways was found to be concentrated around the inboard equatorial plane as suggested by temperature and activation measurements. © 1999 Elsevier Science B.V. All rights reserved.

Keywords: FTU; Disruptions; Limiter; Heat load

1. Introduction

Damage of plasma facing components by disruption generated runaway electrons is of major concern for present and (above all) future tokamak devices like ITER [1]. Runaway production during the startup and steady state phase of the discharge can be limited by carefully adjusting the current ramp-up and gas filling rates, and by controlling the loop voltage. On the contrary, during a disruption, the sudden drop in the electron temperature at the thermal quench leaves the plasma in a high resistive status, which raises the loop voltage to very high values, inductively sustained by the collapsing poloidal magnetic field. The acceleration of the high energy electron tail by this large toroidal electric field can lead to hundreds of MeV electrons hitting the material surfaces inside the vacuum vessel. The extremely localized impact of this runaway beam causes intolerable heat loads with consequent melting and ablation of plasma facing materials. In addition, volumetric heating by these very deeply penetrating electrons can cause serious damage to internal structures such as cooling tubes. Unlike the runaways born in the early phase of the discharge, it is difficult to predict where the disruption generated runaway electrons will strike the in-vessel structures, the outwards shift of their orbits being counteracted by the movement of the plasma column during the current decay.

According to Dreicer's theory [2], the birth rate of runaways during disruptions depends on the values of toroidal electric field E, electron density n_e, electron temperature T_e and Z_{eff} at the end of the thermal quench in such a way that high values of n_e and T_e result in a low creation rate.

The secondary generation mechanism [3] was recently pointed out as the main source of disruption runaways for ITER, where tritium decay or Compton scattering of the gamma rays emitted by the activated wall can provide the initial population of high energy electrons. Secondary generation, which does not depend on the density, is in fact an amplification mechanism: in this sense in the present devices, other sources being negligible, the initial source of runaways is to be searched for in the Dreicer primary generation mechanism.

* Corresponding author. Tel.: +39 6 9400 5695; fax: +39 6 9400 5314; e-mail: maddaluno@frascati.enea.it.

0022-3115/99/$ – see front matter © 1999 Elsevier Science B.V. All rights reserved.
PII: S0022-3115(98)00591-1

When runaway electrons hit the plasma facing materials, (γ, n) photonuclear reactions are induced by the emitted bremsstrahlung radiation, resulting in a photoneutron emission [4–6]. Consequently, a strong hard X-ray emission is always associated with the photoneutron signal at the disruption, as actually observed by the hard X-ray monitors.

In the FTU machine [7], the presence of runaway electrons during the current quench phase of disruptions was previously postulated on the basis of neutron and hard X-ray emissions as well as activation measurements on plasma facing components removed from the inboard side of the vacuum vessel [8]. In the present work a systematic analysis of the photoneutron production during disruptions is reported along with a comparison between experimental results and predicted runaway generation rate according to Dreicer's theory.

2. Experimental apparatus

In FTU the plasma column was limited only by a poloidal limiter prior to 1995, when a full segmented toroidal limiter was installed on the inboard side of the vacuum vessel. The poloidal limiter consisted of two halves: the inner one had a poloidal extension of $\sim$150° and the outer one (removable under vacuum) of $\sim$90°. The toroidal limiter consists of twelve identical sectors with a poloidal extension of $\sim$60°. The outer half of the poloidal limiter is normally used together with the toroidal limiter to protect the outboard side of the vacuum vessel and the radiofrequency waveguides from runaway electrons.

The neutron detector system used for the determination of the photoneutron yield at the disruptions consisted of a set of six calibrated BF_3 proportional counters (5 ms time resolution) located in pairs above the machine on $R = R_0$ circle centered on the tokamak axis [9]. The detectors are calibrated ($\pm$15% uncertainty) for a DD plasma centered at $R = R_0$, while the photoneutron production by runaway electrons takes place in the limiter structures: therefore, the measured photoneutron yields should be multiplied by a corrective factor (evaluated to be of the order of two on JET, see Ref. [6]) in order to obtain the actual yield.

The photoneutron yield was measured by averaging the signals of all detectors which did not saturate during the disruption (the detectors exhibiting different sensitivities): this is a possible source of uncertainty due to the expected toroidal and poloidal asymmetry of the photoneutron emission. The lower and upper detection limits of the detector system were, respectively, $\sim 2 \times 10^9$ and $\sim 5 \times 10^{12}$ neutrons/s.

A faster (100 μs) neutron detector (NE213 scintillator running in the current mode, therefore without n/γ discrimination) was also available, but usually saturated in the disruptions.

The hard X-ray signal was monitored by a standard NaI scintillator also operating in the current mode (0.5 ms time resolution).

The temperature increase in both poloidal and toroidal limiters was monitored by an array of metal-shielded thermocouples embedded within the tiles, with the hot junction at 4 mm beneath the plasma facing surface. In the case of the toroidal limiter, three of the twelve sectors, located at 0°, 180°, and 300° toroidal angles, were instrumented with 44 thermocouples.

3. Results and discussion

A large set of FTU disruptive hydrogen and deuterium discharges was considered, independent of the kind of disruption (density limit, low q, etc.), focusing on the photoneutron production due to runaway electron losses onto the plasma facing components. In this sense, it should be stressed that, contrary to other experiments (TEXTOR [10]), no direct information on runaway electron creation rate is available for FTU. At the onset of the disruptions, the main plasma parameters were in the following ranges: $B_t = 6$T, $I_p = (300\text{–}800)$ kA, $\bar{n}_e = (1\text{–}25) \times 10^{19}$ m^{-3}, $Z_{eff} = 1\text{–}8$. In the discharges with a poloidal limiter, both the inner and outer halves were made of pure or tungsten coated (thickness 2 mm) molybdenum alloy (TZM); in the discharges with a full TZM toroidal limiter, the outer poloidal limiter was made of Inconel.

The leading criterion in screening the discharges being the presence of photoneutrons, the dataset obtained also contains a large number of discharges run with an ill-conditioned machine. Therefore, the dataset does not reflect the usual situation found in an all metal, clean tokamak like FTU, with Z_{eff} strongly decreasing with the increase of the electron density and with physical sputtering as the main mechanism of plasma pollution [11]. Nevertheless, as will be shown later, the lack of photoneutron production and the strong reduction of hard X-ray emission in high density disruptions, usually performed with a well-conditioned machine, suggests that cleanliness and high density play a fundamental role in the reduction of runaway production during disruptions.

From the point of view of photoneutron production, two types of disruptions can be observed in FTU: most of them are abrupt disruptions (with $I_p/(\Delta I_p/\Delta t)_{max}$ of 3–5 ms) and a very small number (<5% of the total) are hesitation disruptions, which show no sudden crash of I_p but a slow decay followed by a plateau phase (with only a slight decrease of I_p), lasting up to 300 ms, ending finally in a hard disruption. In the first case (Fig. 1) a strong photoneutron emission is observed at the

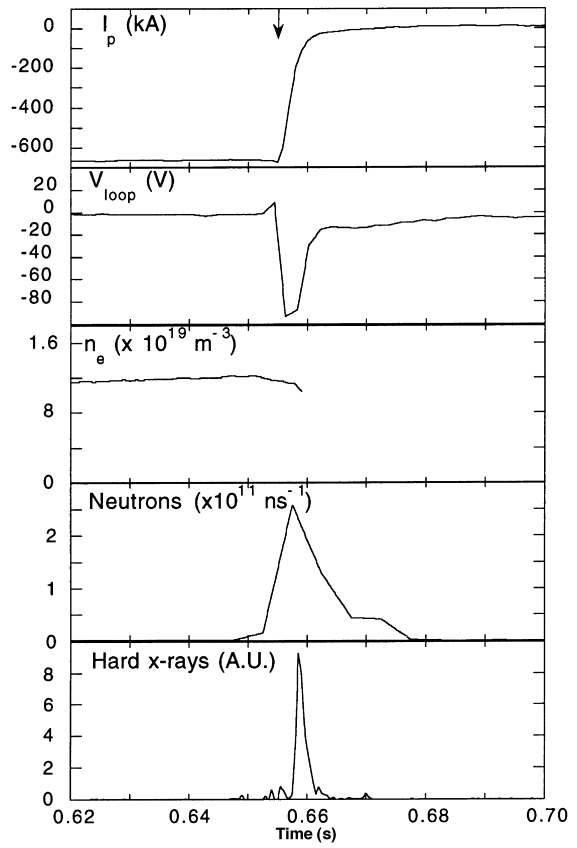

Fig. 1. Typical disruption (the arrow indicates the time of the disruption).

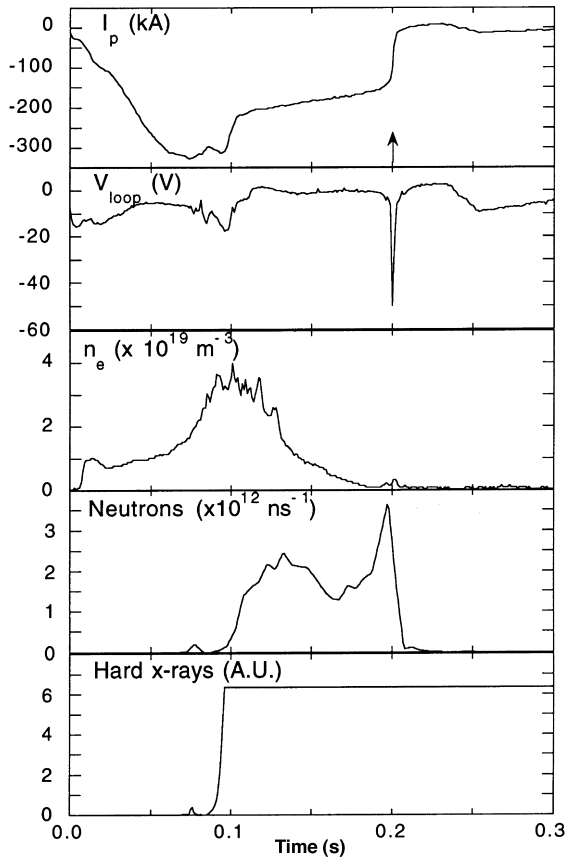

Fig. 2. Hesitation disruption (the arrow indicates the time of the hard disruption).

beginning of the current decay. In the second case (Fig. 2) the photoneutron emission period exactly matches the plateau phase: this phenomenology has already been observed in carbon bounded disruptions in JET [6,12], where it was explained as the result of the current being mainly carried by runaway electrons. Probably the initial slow current decay allows the plasma column to be controlled by the feedback system, thus avoiding the abrupt loss of the runaways on the inboard vessel.

As far as the dependence of the photoneutron yield on plasma parameters is concerned, according to Dreicer's theory the runaway production rate is given by [13]

$$\frac{\mathrm{d}n_\mathrm{r}}{\mathrm{d}t} = n_\mathrm{e} v_\mathrm{e} \lambda, \tag{1}$$

where v_e is the collision frequency of the electrons at the thermal velocity, n_r the runaway electron density and λ is given by

$$\lambda = K(Z_\mathrm{eff})\varepsilon^{-3(Z_\mathrm{eff}+1)/16}\exp\left(-\frac{1}{4\varepsilon}-\sqrt{\frac{Z_\mathrm{eff}+1}{\varepsilon}}\right). \tag{2}$$

In Eq. (2) $K(Z_\mathrm{eff})$ is a weak function of Z_eff and $\varepsilon = E/E_\mathrm{C}$, E being the toroidal electric field and $E_\mathrm{C} \propto n_\mathrm{e}/T_\mathrm{e}$ the critical electric field. As $E = \eta j_0$, η being the Spitzer resistivity and j_0 the central current density (whose profile is assumed to be the same in all discharges), substituting this expression in Eq. (2) the leading term in the runaway production rate is $\exp\left(-\pi a^2 n_\mathrm{e}\sqrt{T_\mathrm{e}}/8Z_\mathrm{eff}I_\mathrm{p}\right)$, where all the quantities refer to the post thermal quench phase (a is the plasma minor radius). However, in our case no reliable measurements were available during the thermal quench. Therefore the values of Z_eff, $\bar{n}_\mathrm{e}$ (line-integrated density) and I_p just before the onset of the thermal quench were used. Moreover, by taking into account that the electron temperature at the end of the thermal quench is related to the plasma current decay time $I_\mathrm{p}/(\Delta I_\mathrm{p}/\Delta t)$ [14], which is about the same for all discharges, the dependence on T_e was disregarded.

The analysis has been performed in ohmic discharges and restricted to disruptions that occurred during the I_p flat-top and not showing runaway behaviour before the disruption (as a result, in the final dataset over 80% of the discharges have $I_\mathrm{p} = 500$ kA). The database mostly

includes toroidal limiter discharges as, unfortunately, just a few flat-top disruptive discharges were found during the short operation with molybdenum or tungsten poloidal limiter, the largest part of them being disruptions occurring during I_p ramp-up with half of them showing current decay hesitation.

The photoneutron yield at the disruption as a function of $\bar{n}_e/Z_{eff}I_p$ is shown in the logarithmic plot of Fig. 3. A linear dependence is found suggesting that the Dreicer runaway generation mechanism is dominant in these disruptions. Irrespective of the other plasma parameters, no photoneutrons were measured in all disruptions occurring at $\bar{n}_e > 1.4 \times 10^{20}$ m^{-3}, although low hard X-ray spikes were sometimes present (except at the highest densities $>2 \times 10^{20}$ m^{-3}). The value of ε below which no photoneutron production was detected is $\sim$0.02 and $\sim$0.05 by assuming post-thermal quench T_e values of 30 and 5 eV, respectively. The hesitation disruptions, not included in Fig. 3, always have very high photoneutron yield ($>0.6 \times 10^{11}$ neutrons). The spread found in the data may be partly due to the above assumption on T_e and to the use of pre-thermal quench values of the quantities appearing in the ratio $\bar{n}_e/Z_{eff}I_p$. However, the main contribution to the data spread is to be attributed to the strong dependence of the photoneutron yield on the runaway electron energy which can vary from shot to shot (as shown below).

The energy of the disruption generated runaway electrons was estimated in two different ways: (a) by γ-ray spectroscopy identification of radionuclides produced by photonuclear reactions in the inboard limiter materials, where only disruption generated runaways are expected to impinge; (b) by integrating the measured loop voltage, V_{loop}, over the duration of the disruption.

In case (a), a lower limit on the runaway energy is given by the energy thresholds of the identified photonuclear reactions, which are in the 7–18 MeV range.

In case (b) the maximum energy is given by $ec \int E\,dt > ec \int (V_{loop}/2\pi R_0)\,dt$, where e and c are, respectively, the electron charge and the speed of light: V_{loop} values in the range 70–150 V were measured corresponding to energies $\sim$15–35 MeV. Such energy values may be increased by about a factor two, reflecting the difference between the measured V_{loop} and the actual voltage at the plasma axis [6].

The typical runaway energy can also be evaluated from the curve of the photoneutron yield per electron vs energy if the number of runaways is known. In hesitation disruptions, where during the I_p plateau phase (when $V_{loop} = 0$) the largest fraction of the current is thought to be carried by the runaway electrons, the number of runaways responsible for the observed photoneutron production can be determined by assuming that the slight I_p decrease in the plateau phase corresponds to an actual loss of runaway electrons onto the limiter. A detailed calculation was performed, following Ref. [6] and the assumptions therein, to determine the photoneutron yield per electron as a function of energy. As the runaway energy inferred from activation measurements (case a) is in the 7–18 MeV range, the calculations were improved with respect to Ref. [6] with an exact evaluation of the integral giving the photoneutron yield per electron, in order to extend the results to the low energy range: in the calculations the runaway electrons were assumed to be stopped in the inboard limiter material (Mo, W), while the bremsstrahlung photons either in the limiter or wall material (Fe). The accuracy of the calculated photoneutron yield per electron was estimated to be of the order of 30%. The results for the three possible material combinations are plotted in Fig. 4. The experimental photoneutron yields per electron determined for some disruptions with Mo poloidal limiter are shown in Fig. 5. Depending on whether the photons were stopped in the limiter (Mo) or in the wall (Fe), runaway energies ranging from 11 to 14 MeV are obtained.

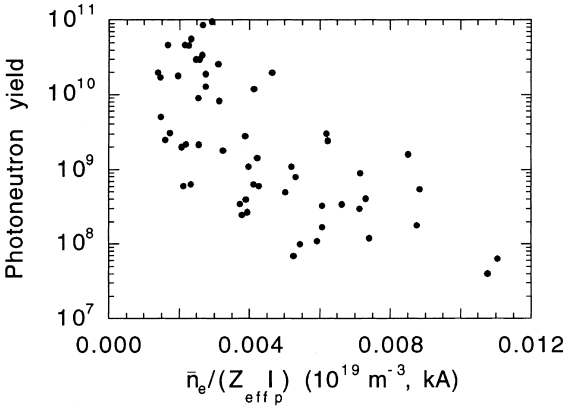

Fig. 3. Photoneutron yield vs. $\bar{n}_e/Z_{eff}I_p$.

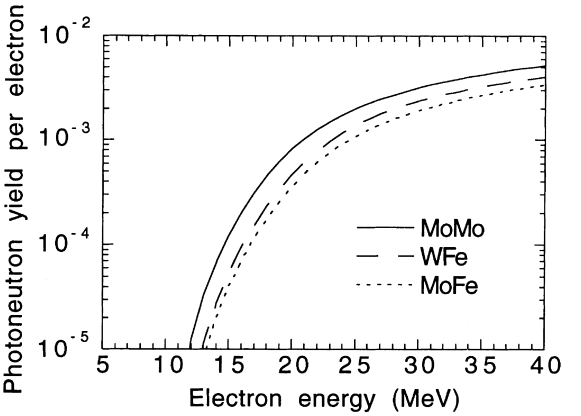

Fig. 4. Photoneutron yield per electron vs. energy (the first element in the labels denotes the electron stopping material, the second one the photon stopping material).

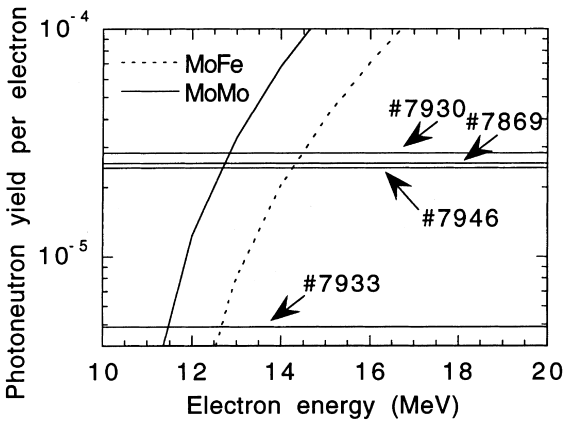

Fig. 5. Runaway energy determination in some hesitation disruptions.

The range of runaway electron energies (at fixed $\bar{n}_e/Z_{eff}I_p$) estimated for FTU can easily account for a two order of magnitude spread in the photoneutron yield: this is actually consistent with that observed in Fig. 3.

As far as the secondary generation mechanism is concerned, an evaluation [15] of the expected grow rate $(1/J_r)$ (dJ_r/dt) of the resulting runaway current J_r leads, for the range of plasma currents considered, to a number of e-folds during avalanche from 0.6 to 2, corresponding to an amplification factor from 2 to 7. Therefore, the effect of this generation mechanism on our photoneutron production measurements is not expected to be particularly relevant, compared to the above mentioned photoneutron yield spread of a factor $\sim$100.

The damage by runaway electrons on the inboard side of the vacuum vessel is expected to be only produced during disruptions, as runaways lost during the steady state portion of the discharge normally hit the outboard poloidal limiter (due to the effect of drift orbit shift). As a matter of fact, molten activated zones were found on the equatorial regions of the inboard limiters [8]. An abnormal temperature increase, ΔT, was recorded by thermocouples embedded within the equatorial tiles of the toroidal limiter (preferentially in sector 7) or of the inboard poloidal limiter, only in discharges ending with a disruption characterized by a large amount of photoneutrons.

A rough estimate of the thermal load by electrons pushed on the inboard toroidal limiter during the collapse of the plasma column was made for one of these discharges (photoneutron yield $\sim 1.7 \times 10^{11}$), for which a clear image of the impact zone was available from a CCD camera [16] and strong molybdenum emission lines were also recorded. The $\Delta T = 76$°C measured on the hit tile was related to the energy load E_{Tot} by N_r runaways of average energy E_r impinging on the limiter. The best agreement between the photoneutron yield per electron $N_{photoneutrons}/(E_{Tot}/E_r)$ calculated by using the experimental values of $N_{photoneutrons}$ and E_{Tot} and the one inferred from the curve in Fig. 4 was found for E_r ranging between 13 and 16 MeV.

4. Conclusions

Photoneutron production during disruptions in FTU was monitored by a set of calibrated BF_3 proportional counters.

The dependence of the experimental photoneutron yield on Z_{eff}, n_e and I_p is in agreement with the Dreicer mechanism being the primary source of runaway electrons during FTU disruptions.

At electron density $\bar{n}_e > 1.4 \times 10^{20}$ m^{-3} (corresponding to Z_{eff} close to 1) no photoneutrons were detected, suggesting that in disruptions occurring in high density clean discharges the runaway production is either absent or very low (the runaways are a fraction $<10^{-9}$ of the thermal electrons).

The possible presence of an amplification of the runaway population by the secondary generation mechanism could not be checked on the basis of the present neutron measurements. However, this effect should not be large, owing to the rather low plasma current values.

Diagnostics capable of measuring runaways parameters while they still are confined (such as thermography) are strongly desirable to be improved on FTU.

References

[1] A.J. Russo, R.B. Campbell, Nucl. Fusion 33 (1993) 1305.
[2] H. Dreicer, Phys. Rev. 115 (1959) 238.
[3] R. Jayakumar, H.H. Fleischmann, S. Zweben, Phys. Lett. A 172 (1993) 447.
[4] W.C. Barber, W.D. George, Phys. Rev. 116 (1959) 1551.
[5] M.J. Berger, S. M Seltzer, Phys. Rev. C 2 (1970) 621.
[6] O.N. Jarvis, G. Sadler, J.L. Thompson, Nucl. Fusion 28 (1988) 1981.
[7] R. Andreani et al., Fusion Technology, Proceedings of the 16th Symposium, vol. 1, North-Holland, Amsterdam, 1990, p. 218.
[8] G. Maddaluno, F. Pierdominici, M. Vittori, J. Nucl. Mater. 241–243 (1997) 908.
[9] L. Bertalot, B. Esposito, S. Podda, S. Rollet, Rev. Sci. Instr. 63 (1992) 4554.
[10] R. Jaspers et al., Nucl. Fusion 36 (1996) 367.
[11] M.L. Apicella et al., Nucl. Fusion 37 (1997) 381.
[12] G.R. Harris, Report JET-R(90)07 (1990).
[13] R. Jaspers et al., Nucl. Fusion 33 (1993) 1775.
[14] R. Yoshino, J. Nucl. Mater. 220-222 (1995) 132.
[15] M.N. Rosenbluth, S.V. Putvinski, Nucl. Fusion 37 (1997) 1355.
[16] R. De Angelis, private communication, 1998.